A Simulation Study for Optimal Pinhole Collimator Design in Gamma Camera Systems

M. A. Ghoneim

Department of Physics, Faculty of Science, New Valley University, El-Kharja, Egypt

Abstract

Background: The usage of a semiconductor detector with a pinhole collimator can provide high spatial resolution due to its high intrinsic resolution. However, the collimator system has low sensitivity due to the hole's small diameter. Therefore, the optimization between the spatial resolution and sensitivity is critical for determining the image quality in the gamma camera system. **Aims and Objectives:** A pinhole collimator was designed and simulated to achieve the desired level of resolution and sensitivity in a gamma camera by utilizing a CdTe semiconductor detector. **Materials and Methods:** To conduct this objective, a simulation toolkit based on the Geant4 Application for Tomographic Emission (GATE) was employed. The imaging capabilities of the proposed system were assessed by varying the magnification factor and pinhole diameter to estimate spatial resolution and sensitivity. Moreover, a hot rod phantom was designed to evaluate the system's overall imaging functionality. **Results:** Results revealed that an increase in the pinhole diameter was correlated with an increase in sensitivity, while the spatial resolution was decreasing. There were distinct variations in sensitivity and spatial resolution depending on changes in the magnification factor as well. Finally, by analyzing trade-off curves, 1.38±0.081 mm was approximately the optimal pinhole diameter for our proposed system. **Conclusion:** The optimum position for a pinhole collimator with a CdTe semiconductor detector was demonstrated.

Keywords: Gamma camera, magnification factor, pinhole collimator, sensitivity, spatial resolution

Received on: 26-07-2024 **Review completed on:** 21-09-2024 **Accepted on:** 14-10-2024 **Published on:** 18-12-2024

Introduction

The fields of nuclear medicine technology provide valuable insights into both functional and anatomical aspects of physiological processes. This has led to an increased recognition of its significance in the diagnostic imaging field.[1-4]

Nuclear medicine imaging has two primary types of devices: positron emission tomography (PET), without photon collimating, and single-photon emission computed tomography (SPECT) or the gamma camera with photon collimating. The gamma camera, or SPECT, generally employs a mono-energetic gamma source, such as the widely used ^{99m}Tc (half-life of 6.02 h and 140 keV photon energy peak).[5-8] NaI (Tl) scintillation camera detectors and traditional or recently created semiconductor detectors made of silicon (Si) or germanium (Ge) are frequently utilized in the field of nuclear medicine. However, both typical Si and Ge semiconductor and NaI (Tl) scintillation detectors have drawbacks due to their low detection efficiencies and their low intrinsic resolution. Si and Ge semiconductors are expensive and need more cooling systems as well.[9-11] In recent years, to overcome these limitations, cadmium telluride (CdTe) and cadmium zinc telluride (CZT) semiconductor detectors were developed. These detectors do not require any cooling devices that can detect gamma rays at room temperatures. The main benefits of CZT and CdTe detectors include around 3%–6% better energy resolution in the case of ^{99m}Tc (140 keV photon energy peak), high sensitivity resulting from their high detection and counting efficiency, and their good spatial resolution due to the intrinsic resolution being equivalent to the pixel size.[12-21]

In this context, by including CZT and CdTe semiconductor detectors, gamma cameras can solve and enhance the

Access this article online	
Quick Response Code:	Website: www.jmp.org.in
	DOI: 10.4103/jmp.jmp_127_24

Address for correspondence: Dr. M. A. Ghoneim, Department of Physics, Faculty of Science, New Valley University, El-Kharja 72714, Egypt. E-mail: ghoneim20m@gmail.com

How to cite this article: Ghoneim MA. A Simulation study for optimal pinhole collimator design in gamma camera systems. J Med Phys 2024;49:648-53.

embedded image quality restrictions (such as sensitivity and spatial resolution) for traditional gamma cameras using NaI (TI) scintillation detectors and Si or Ge semiconductors.

Collimators are essential in nuclear medicine imaging through two different ways when used them in gamma cameras or SPECT systems. First, they selectively absorb emitted gamma rays from the body to create the imaging, making it crucial to determine the direction of gamma rays. Second, by employing collimators, gamma cameras can eliminate scattered photons and mispositioned gamma rays. Thus, gamma cameras carry out a selective absorption for incoming photons. For these factors, the design of collimators has a significant impact on the image quality, including sensitivity and spatial resolution.[22-27] Pinhole collimators with a specific geometry can be employed in preclinical gamma camera systems to obtain a better spatial resolution and magnification effects, especially with detectors based on CZT or CdTe semiconductor materials. The magnification effects have a direct effect on intrinsic resolution, which makes pinhole collimators suitable for small objects like the thyroid. Furthermore, the sensitivity of pinhole imaging systems is improved as the pinhole's distance from the object being imaged is reduced.[28,29] However, a major limitation of pinhole collimators is their reduced sensitivity. As the collimator hole size is small, enhancing spatial resolution leads to a loss of sensitivity in the system.[30,31] Thus, it is crucial to achieve optimized image quality that produces an acceptable compromise between spatial resolution and sensitivity.

To achieve this investigation, a Geant4 Application for Tomographic Emission (GATE) simulation is conducted to assess spatial resolution and sensitivity using a PID 350 (AjatOy Ltd., Finland) CdTe semiconductor detector. Moreover, the system is optimized using a pinhole collimator and that simulated detector through varying the pinhole collimator diameters and magnification factors. Finally, a simulated phantom was designed to confirm the overall image performance.

Materials and Methods

To evaluate the impact of the magnification factor and pinhole diameter on image quality, Monte Carlo simulations were carried out using GATE 9.1 (GEANT4 Application for Tomographic Emission) is an open-source toolkit based on the Geant4 (GEometry ANd Tracking) platform for Monte Carlo simulations in medical imaging and radiotherapy. The OpenGATE collaboration institutions (laboratories, companies, and medical centers) are in Lyon, France. (Available from: http://www.opengatecollaboration.org/). GATE is built by the native GEANT4 code and is well-dedicated for modeling nuclear medicine systems such as planar gamma cameras, SPECT, and PET.[32-37]

Using the GATE tool, a PID 350 CdTe semiconductor detector was simulated in this work. The employed CdTe semiconductor detector had a thickness of 3 mm, a total size of 44.8 mm × 44.8 mm, pixel sizes of 0.35 mm × 0.35 mm, and a matrix size of 128 × 128. At a gamma photon energy of ^{99m}Tc (140 keV), the counting efficiency and density of a 3 mm thick CdTe and Si semiconductor, and NaI (TI) scintillation detectors are illustrated in Table 1. The 76% counting efficiency of the 3 mm thick CdTe semiconductor detector was demonstrated to be better. In comparison to Si semiconductors and NaI (TI) scintillation detectors, the efficiency of CdTe semiconductors was 7.6 and 1.4 times greater, respectively. Due to their high density and atomic number, CdTe semiconductor detectors are more efficient than other detectors.[38]

The pinhole collimator is a single-aperture, cone-shaped instrument that is typically made of heavy materials like lead or tungsten because of its low cost and suitable stiffness. In recent times, many studies have been carried out on alternative collimator materials, such as uranium and gold. However, their high manufacturing costs and limited availability make them less practical options.[39-41] Therefore, in this study, tungsten is nominated as the material for the pinhole collimator.

Figure 1 presents a diagram of the pinhole collimator for this simulation. This simulation involved three different source-to-aperture distances, specifically 5, 10, and 15 cm, while maintaining a fixed aperture-to-detector distance of 30 cm. The pinhole's diameter ranged from 0.2 up to 2 mm, and the acceptance angle of the pinhole collimator was set at 51°. The following formulas were used to determine the system's geometric efficiency or sensitivity (g) and spatial resolution R_{system}:[42]

Table 1: The density and counting efficiency at 140 keV gamma photon energy of 3 mm-thick materials for various detectors

Materials	CdTe	Silicon	NaI (TI)
Counting efficiency (%)	76	10	54.3
Density (g/cm^3)	5.85	2.33	3.67

CdTe: Cadmium telluride

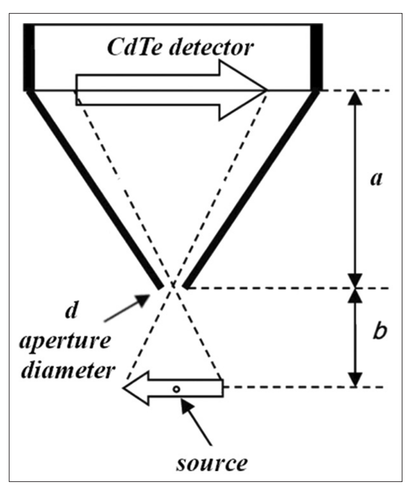

Figure 1: Pinhole collimator diagram for this work

$$R_{system} = \sqrt{\left(R_{intrinsic}^2 + R_{collimator}^2\right)} \quad (1)$$

$$R_{intrinsic} = \frac{pixelsize}{magnificationfactor} \quad (2)$$

$$d_{effective} = \sqrt{d\left(d + \frac{2}{\mu}tan\left(\frac{\theta}{2}\right)\right)} \quad (3)$$

$$R_{collimator} = \frac{d_{effective}\left(a+b\right)}{a} \quad (4)$$

$$g = \frac{d_{effective}^2 cos^3\theta}{16b^2} \quad (5)$$

where, $R_{intrinsic}$ is the intrinsic resolution of the detector, $R_{collimator}$ is the resolution of collimator, (a) is the pinhole aperture-to-the detector distance, (*b)* is the distance from the source to collimator's aperture, $d_{effective}$ is the effective diameter of the pinhole, (*d)* is the pinhole diameter, (μ*)* is the linear attenuation coefficient of the pinhole collimator material, and (θ*)* is the acceptance angle of the pinhole aperture. The calculation for the magnification factor is a/b. $R_{intrinsic}$ was 0.35 mm in this work. The effective diameter of the pinhole $d_{effective}$ is a little bigger than the actual diameter (*d),* due to the gamma rays penetrating the aperture's edges.[43] According to Eq. (3), the pinhole's effective diameter is dependent on the pinhole aperture's acceptance angle as well as the material of the pinhole (the linear attenuation coefficient). The effective pinhole diameter increases as the linear attenuation coefficient decreases and the acceptance angle increases.[44] Therefore, the system resolution and sensitivity are significantly impacted by these parameters.

A hot rod phantom was simulated to verify the image performance, as depicted in Figure 2. The phantom had six rod-shaped areas, each having different diameters and filled with a different activity of ^{99m}Tc [All were written on the diagram in Figure 2]. A water solution of ^{99m}Tc was used to fill the phantom. The phantom included different diameters: a small rod to mimic the small organs sizes (e.g., in neurologic applications and brain imaging, spatial resolution is below 1 mm) and a large one to represent the organs' greater size (e.g., in thyroid nodules, imaging is 2–3 mm in size).[45,46] Phantom activities were chosen to assess the system sensitivity as the animal organs have different responses to radioactive material.

In this work, the image spatial resolution and sensitivity were estimated to evaluate the performance of proposed pinhole systems. A ^{99m}Tc point source was used to assess image performance, with an activity of 1 MBq and an acquisition time of 900 s. For each of magnification factors 2, 3, and 6, the pinhole collimator's diameter was changed by increments of 0.2 mm up to a maximum of 2 mm. Counts per second per kBq (cps/kBq) were used to measure the sensitivity, and the Full Width at Half Maximum (FWHM) of the point spread

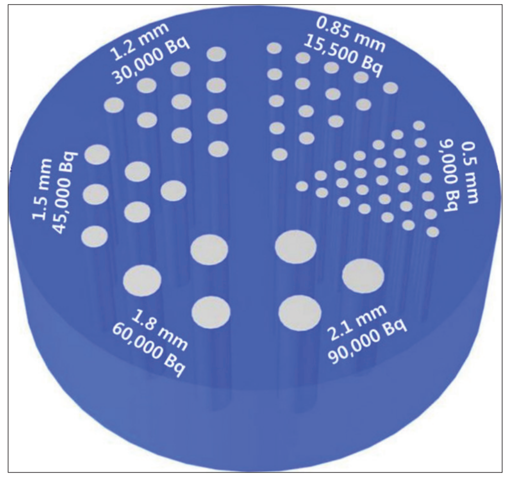

Figure 2: Phantom diagram for this study

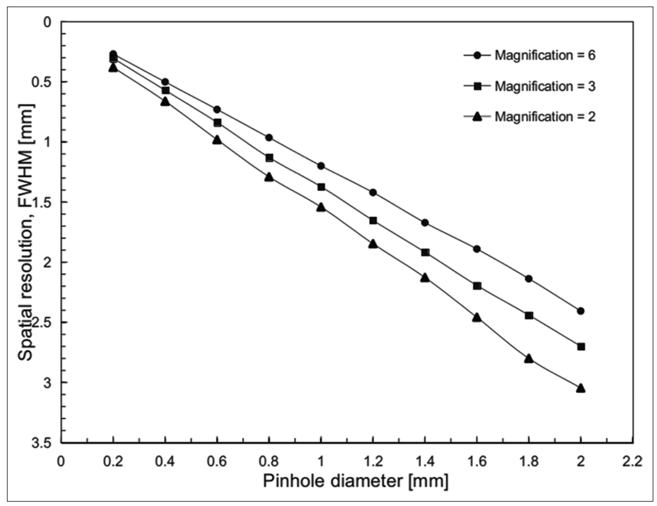

Figure 3: Estimated spatial resolutions with collimator diameters for three different magnification factors

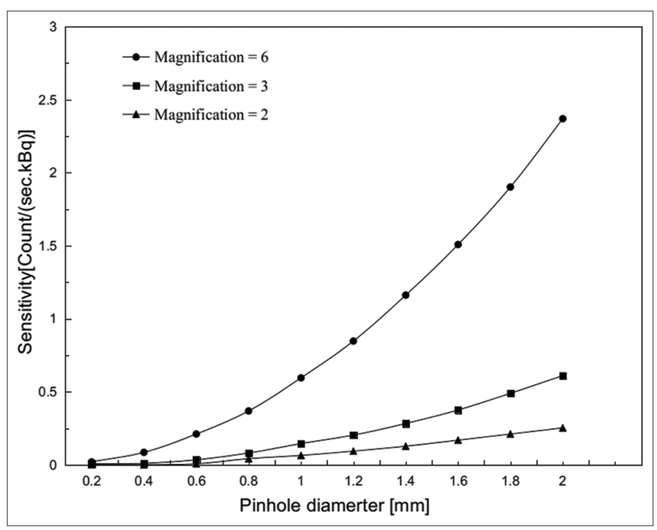

Figure 4: Estimated sensitivities with collimator diameters for three different magnification factors

function was used to calculate the spatial resolution. Finally, trade-off curves were plotted to optimize the collimating system's design, which expresses the relationship between sensitivity and spatial resolution, considering the magnification factors and the pinhole's aperture diameters. The source-to-aperture distance is changeable in pinhole collimators, while the aperture-to-detector distance remains constant. To obtain a better magnification factor, the source-to-aperture distance should be small. Thus, the choice of 2, 4, and 6 cm is acceptable and variable to assess the most of quality control tests.[47]

Results and Discussion

The spatial resolution and sensitivity were evaluated by varying the collimator diameters for each magnification factor (2, 3, and 6), and then the results were plotted, as shown in Figures 3 and 4.

Figure 3 shows a gradual increase (e. g., from 0.2 to 2.41 mm with a 6 magnification factor with uncertainty ranging from 1.3×10^{-3} to 0.024 mm, respectively) in spatial resolution or FWHM with a pinhole diameter for all magnification factors. Figure 4 shows an improvement (e. g., from 0.02 to 2.37 counts/s KBq with a 6 magnification factor with uncertainty ranging from 3.4×10^{-3} to 0.012 counts/s KBq, respectively) in the measured sensitivity with a pinhole diameter for all magnification factors. The increase in the spatial resolution with a pinhole diameter can be attributed to the increase in field of view (acceptance angle) and the number of counted photons falling within the detector. According to Equations (3 and 4), the effective diameter of the pinhole increases as its acceptance angle increases. Gamma rays that reach the detector then rise. Thus, resolution of the system increases. In addition, Equation (5) shows that the geometric efficiency or sensitivity of the system is directly affected by the effective diameters as well. As a result, the system becomes more sensitive as the effective diameter increases. The results revealed that as magnification factors increased, both spatial resolution and sensitivity improved. A high value of the magnification factor means, at a stable aperture-to-detector distance, a decrease in the source-to-aperture distance. This leads to better spatial resolution and geometric efficiency. The effect of the magnification factor on spatial resolution was provided by Williams *et al*.[47] However, since most typical gamma camera systems employ collimators, obtaining high sensitivity and high spatial resolution simultaneously is difficult. For instance, in cardiac studies, the acquisition time typically takes 20 min. This is a comparatively long acquisition time and requires the use of highly sensitive collimators. However, the use of highly sensitive collimators in cardiac acquisitions causes a degradation in spatial resolution. Therefore, trade-off curves are plotted in Figure 5 between spatial resolution and sensitivity as a function of pinhole diameter to identify the optimal pinhole design (using different collimator diameters and a fixed magnification factor). In general, pinhole collimators come with multiple pinhole inserts with different diameters. Smaller-diameter holes provide better resolution. For the clinical applications, Connolly *et al*. illustrated that the pinholes of 2–3-mm diameter provide images of 100–300 kcounts with better anatomic detail for a child's acquisition.[48] A further reduction in pinhole diameter would result in improved resolution that is clinically significant.

Based on the graph in Figure 5, the observations revealed that the optimum pinhole diameter was around 1.38 ± 0.081 mm (This value was obtained using the standard deviation of the mean of the intersection points of the trade-off between

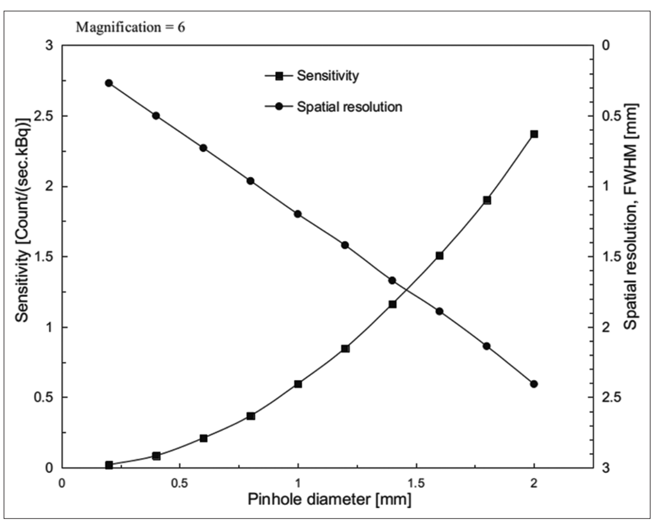

Figure 5: Optimal pinhole diameter based on spatial resolution and sensitivity for each magnification factor 6, 3, and 2 (graphs of factors 3 and 2 not shown)

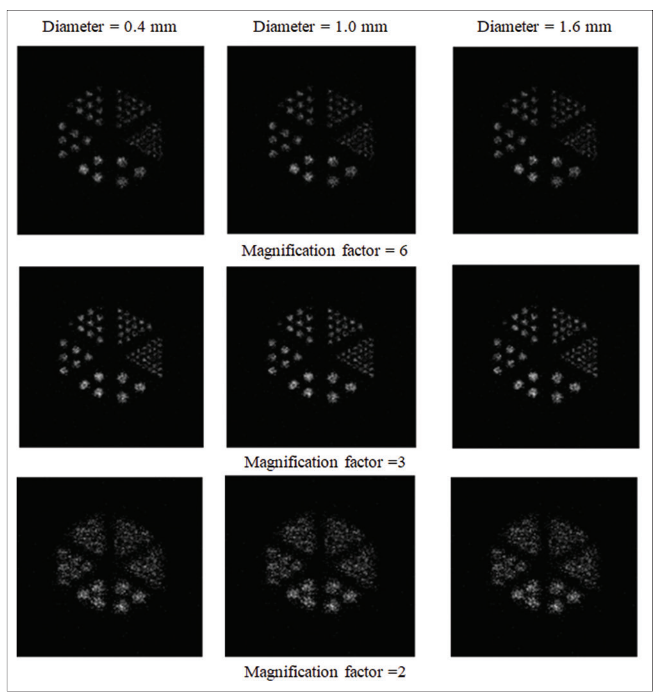

Figure 6: The obtained phantom images of hot rods (with different magnification factors and pinhole collimator diameters)

the sensitivity and spatial resolution graphs shown above), regardless of magnification factor variations. A similar behavior was reported by Song *et al*.:[49] the trade-off curves of sensitivity and spatial resolution approximated as a function of the pinhole diameter. In their analysis, they found that the optimal range for pinhole diameter was between 1 and 1.5 mm for the system configuration.

Figure 6 shows the hot rod phantom images that have been used to verify the overall image performance. Pinhole collimator diameters of 1.6, 1.0 and 0.4 mm, with magnification factors of 6, 3 and 2 were applied to acquire phantom images. As a result of this study, at all magnification factors, all rods with diameters of 0.85, 1.2, 1.5, 1.8, and 2.1 mm were resolvable. However, there are differences in spatial resolution and sensitivity as the pinhole diameter changes. Sensitivity improved as pinhole diameter increased, while spatial resolution degraded. By increasing the diameter of the pinhole, the geometric efficiency can be increased. However, the pinhole collimator resolution degrades due to the increased effective pinhole diameter. Therefore, determining the pinhole diameter requires compromises between spatial resolution and sensitivity. When the pinhole diameter was 0.4 mm and the magnification factor was 6, the smallest 0.5 mm rods were resolved. These phantom results indicated that the spatial resolution of the phantom image and our suggested system are the same.

Conclusion

Using a GATE simulation, a dedicated pinhole collimator was developed for gamma camera systems with a CdTe semiconductor detector. Sensitivity and spatial resolution were measured by verifying magnification factors and pinhole diameters. Finally, a hot rod phantom was employed to estimate the general image quality and performance. The results demonstrated that the best image performance was acquired with a pinhole diameter of approximately 1.38 ± 0.081 mm at all magnification factors, providing a good compromise between spatial resolution and sensitivity for our proposed system.

Financial support and sponsorship

Nil.

Conflicts of interest

There are no conflicts of interest.

References

1. Hussain S, Mubeen I, Ullah N, Shah SSUD, Khan BA, Zahoor M, *et al*. Modern diagnostic imaging technique applications and risk factors in the medical field: a review. BioMed research international 2022;2022.1:1-19. Available from: https://doi.org/10.1155/2022/5164970.
2. Even-Sapir E, Keidar Z, Bar-Shalom R. Hybrid imaging (SPECT/CT and PET/CT) improving the diagnostic accuracy of functional/metabolic and anatomic imaging. Semin Nucl Med 2009;39:264-275. WB Saunders.
3. Histed SN, Lindenberg ML, Mena E, Turkbey B, Choyke PL, Kurdziel KA. Review of functional/anatomic imaging in oncology. Nuclear medicine communications 2012;33:349.
4. Wong KK, Fortino G, Abbott D. Deep learning-based cardiovascular image diagnosis: a promising challenge. Future Generation Computer Systems 2020;110:802-811.
5. Iskandrian AE, Hage FG. eds. Nuclear Cardiac Imaging: Principles and Applications. Oxford University Press, USA, Incorporated, 2024;61-86. Available from: https://doi.org/10.1093/med/9780190095659.001.0001.
6. Ghoneim MA, Khedr MH, Elshemey WM. Geometrical parameters and scattered radiation effects on the extrinsic sensitivity and counting efficiency of a rectangular gamma camera. Applied Radiation and Isotopes 2016;118:31-135.
7. Elshemey WM, Ghoneim MA, Khader MH. Scattered radiation effects on the extrinsic sensitivity and counting efficiency of a gamma camera. Applied Radiation and Isotopes 2013;77:18-22.
8. Rowland DJ, Cherry SR. Small-animal preclinical nuclear medicine instrumentation and methodology. In Seminars in nuclear medicine 2008;38:No. 3:209-222. WB Saunders.
9. Niknami M, Valipour M. Compton Imaging Systems Based on Semiconductor Detectors. In Gamma Ray Imaging: Technology and Applications. Cham: Springer International Publishing 2023. p. 65-86.
10. Owens A. Photoconductive Materials. In Photoconductivity and Photoconductive Materials; John Wiley and Sons ltd.: Hoboken, NJ, USA, 2022;2022:399–491.
11. Green MV, Seidel J, Vaquero JJ, Jagoda E, Lee I, Eckelman WC. High resolution PET, SPECT and projection imaging in small animals. Computerized medical imaging and graphics 2001;25:79-86.
12. Opanasyuk A, Kurbatov D, Znamenshchykov Y, Diachenko O, Ivashchenko M. CdTe-/CdZnTe-Based Radiation Detectors. In Handbook of II-VI Semiconductor-Based Sensors and Radiation Detectors: Vol. 3: Sensors, Biosensors and Radiation Detectors. Cham: Springer International Publishing 2023. p. 35-73
13. Roy UN, Camarda GS, Cui Y, Yang G, James RB. Impact of selenium addition to the cadmium-zinc-telluride matrix for producing high energy resolution X-and gamma-ray detectors. Scientific Reports, 2021;11:10338.
14. Roy UN, Camarda GS, Cui Y, James RB. Advances in CdZnTeSe for radiation detector applications. Radiation 2021;1:123-130.
15. Abbaspour S, Mahmoudian B, Islamian J. Cadmium telluride semiconductor detector for improved spatial and energy resolution radioisotopic imaging. World journal of nuclear medicine 2017;16:101-107.
16. Sordo SD, Abbene L, Caroli E, Mancini AM, Zappettini A, Ubertini P. Progress in the development of CdTe and CdZnTe semiconductor radiation detectors for astrophysical and medical applications. Sensors 2009;9:3491-3526.
17. Scheiber C. New developments in clinical applications of CdTe and CdZnTe detectors. Nuclear Instruments and Methods in Physics Research Section A: Accelerators, Spectrometers, Detectors and Associated Equipment 1996;380:385-391.
18. Abe A, Takahashi N, Lee J, Oka T, Shizukuishi K, Kikuchi T, *et al*. Performance evaluation of a hand-held, semiconductor (CdZnTe)-based gamma camera. European journal of nuclear medicine and molecular imaging 2003;30:805-811.
19. Takahashi T, Watanabe S. Recent progress in CdTe and CdZnTe detectors. IEEE Transactions on nuclear science 2001;48:950-959.
20. Iida H, Ogawa K. Comparison of a pixelated semiconductor detector and a non-pixelated scintillation detector in pinhole SPECT system for small animal study. Annals of nuclear medicine 2011:25:143-150.
21. Ogawa K, Ohmura N, Iida H, Nakamura K, Nakahara T, Kubo A. 2009. Development of an ultra-high resolution SPECT system with a CdTe semiconductor detector. Ann Nucl Med 2009;23:763–770. Available from: https://doi.org/10.1007/s12149-009-0293-x.
22. Cerbone LA, Cimmino L, Sarno A, Biesuz NV, Bolzonella, R, Mettivier G, *et al*. Monte Carlo and experimental evaluation of a Timepix4 compact gamma camera for coded aperture nuclear medicine imaging with depth resolution. Physica Medica 2023;113:102663.
23. Mahani H, Raisali G, Kamali-Asl A, Ay MR. Spinning slithole collimation for high-sensitivity small animal SPECT: Design and assessment using GATE simulation. Physica Medica 2017;40:42-50.
24. Mikeli M, Thanasas D, Stiliaris E. Collimator Study of a γ-Camera System using GATE. IEEE Nuclear Science Symposium Conference

Record 2009. p. 3931-3935. DOI: 10.1109/NSSMIC.2009.5401940.
25. Moore SC, Kouris K, Cullum I. Collimator design for single photon emission tomography. European journal of nuclear medicine 1992;19:138-150.
26. Lee Y, Kim H. Comparison of a newly-designed stack-up collimator with conventional parallel-hole collimators in pre-clinical CZT gamma camera systems: A montecarlo simulation study. J Korean Phy Soc 2014;65:1149-1158.
27. Wieczorek H, Goedicke A, Edstrom F, Degenhardt C, Botterweck H. Bippus R. 2005. Collimator spatial resolution. In IEEE Nuclear Science Symposium Conference Record, 2005;3:1-5. DOI: 10.1109/NSSMIC.2005.1596651.
28. Mok SP, Wang Y, Tsui BMW Design of a novel pinhole collimator system for SPECT imaging of small animals with different sizes. IEEE Nucl Sci Sympos Conf Record M 11-285: 2005. p. 2649-2652.
29. Nolte T, Gross-Weege N, Schulz V. (Hybrid) SPECT and PET technologies. In Molecular Imaging in Oncology; Schober O, Kiessling F, Debus J, Eds.; Recent Results in Cancer Research; Springer: Cham, Switzerland, 2020;216:111–133.
30. Lukas M, Kluge A, Beindorff N, Brenner W. Multi-isotope capabilities of a small-animal multi-pinhole SPECT system. Journal of Nuclear Medicine 2020;61:152-161.
31. Ishizu K, Mukai T, Yonekura Y, Pagani M, Fujita T, Magata Y, *et al*. Ultra-high resolution SPECT system using four pinhole collimators for small animal studies. Journal of Nuclear Medicine 1995;36:2282-2287.
32. Auer B, Könik A, Fromme TJ, De Beenhouwer J, Kalluri KS, Lindsay C, *et al*. Mesh modeling of system geometry and anatomy phantoms for realistic GATE simulations and their inclusion in SPECT reconstruction. Physics in Medicine and Biology 2023;68:1-32. Available from: https://doi.org/10.1088/1361-6560/acbde2.
33. Sadremomtaz A, Telikani Z. Validation and optimization studies of small animal SPECT using GATE Monte Carlo simulation. Nuclear Instruments and Methods in Physics Research Section A: Accelerators, Spectrometers, Detectors and Associated Equipment. 2019;915:94-101.
34. Jan S, Benoit D, Becheva E, Carlier T, Cassol F, Descourt P, *et al*. GATE V6: a major enhancement of the GATE simulation platform enabling modelling of CT and radiotherapy. Physics in Medicine and Biology 2011;56:881.
35. Staelens S, Strul D, Santin G, Vandenberghe S, Koole M, D'Asseler Y, *et al*. Monte Carlo simulations of a scintillation camera using GATE: validation and application modelling. Physics in Medicine and Biology 2003;48:3021.
36. Buvat I, Lazaro D. Monte Carlo simulations in emission tomography and GATE: An overview. Nuclear Instruments and Methods in Physics Research Section A: Accelerators, Spectrometers, Detectors and Associated Equipment, 2006;569:323-329.
37. Assie K, Breton V, Buvat I, Comtat C, Jan S, Krieguer M, *et al*. Monte Carlo simulation in PET and SPECT instrumentation using GATE. Nuclear Instruments and Methods in Physics Research Section A: Accelerators, Spectrometers, Detectors and Associated Equipment, 2004; 527:180-189.
38. Lee Y, Kang W. Performance evaluation of high-resolution square parallel-hole collimators with a CZT room temperature pixelated semiconductor SPECT system: a Monte Carlo simulation study. Journal of Instrumentation 2015;10:T07004.
39. Han DH, Lee SJ, Kim JO, Kwon DE, Jung KH, Baek CH. Optimization of the design parameters for a thyroid care nuclide monitoring diverging collimator using Monte Carlo simulation. Journal of the Korean Physical Society 2022;81:675-679.
40. Lee YJ, Ryu HJ, Lee SW, Park SJ. Kim HJ. Comparison of ultra-high-resolution parallel-hole collimator materials based on the CdTe pixelated semiconductor SPECT system. Nuclear Instruments and Methods in Physics Research Section A: Accelerators, Spectrometers, Detectors and Associated Equipment, 2013;713:33-39.
41. Smith MF, Jaszczak RJ, Wang H, Li J. Lead and tungsten pinhole inserts for I-131 SPECT tumor imaging: experimental measurements and photon transport simulations. IEEE Transactions on Nuclear Science 1997;44:74-82.
42. Smith MF, Kieper DA, Majewski S, Weisenberger AG, Welch B. Optimizing pinhole and parallel hole collimation for scintimammography with compact pixellated detectors. IEEE T Nucl Sci 2003;50:321-324.
43. Anger HO. Radioisotope cameras. 1965;1:14-46, California Digital Library, University of California. Available from: https://escholarship.org/uc/item/4k362467.
44. Bom V, Goorden M, Beekman F. Comparison of pinhole collimator materials based on sensitivity equivalence. Physics in Medicine and Biology 2011;56:3199.
45. Franc BL, Acton PD, Mari C, Hasegawa BH. Small-animal SPECT and SPECT/CT: important tools for preclinical investigation. Journal of nuclear medicine 2008;49:1651-1663.
46. Sabih D, Kashif R. Thyroid nodule imaging, Status and limitations. Asia Oceania J Nucl Med Biol 2015;3:50-57.
47. Williams MB, Stolin AV, Kundu BK. Investigation of efficiency and spatial resolution using pinholes with small pinhole angle. IEEE Transactions on Nuclear Science 2003;50:1562-1568.
48. Connolly LP, Treves ST, Davis RT, Zimmerman RE. Pediatric applications of pinhole magnification imaging. Journal of Nuclear Medicine 1999;40:1896-1901.
49. Song TY, Choi Y, Chung YH, Jung JH, Choe YS, Lee KH, *et al*. Optimization of pinhole collimator for small animal SPECT using Monte Carlo simulation. IEEE Transactions on Nuclear Science 2003;50:327-332.